PROCEEDINGS OF SCIENCE

Measurements of multi-boson production including vector-boson scattering at ATLAS

Xiaotian Liu*, **on behalf of the ATLAS Collaboration**

University of Science and Technology of China,
No.96 Jinzhai Road, Hefei, China

E-mail: xiaotian.liu@cern.ch

Measurements of multi-boson production at the LHC provide a precision test of the electroweak gauge structure predicted by the Standard Model, and they also offer a unique window to new physics beyond the SM. In this proceeding, we present recent ATLAS measurements on multi-boson productions, including the electroweak production of a $Z\gamma$ pair in association with two jets, the first observation of three W bosons production, the observation of the W pair production in photon-induced collisions, and also differential measurements of the inclusive four-lepton production. Interpretations on BSM using those precision measurements are also discussed. Moreover, constraints on Wilson coefficients of the SM Effective Field Theory are obtained by a combined fit to several multi-boson cross-section measurements.

7th Symposium on Prospects in the Physics of Discrete Symmetries (DISCRETE 2020-2021)
29th November - 3rd December 2021
Bergen, Norway

*Speaker

© Copyright owned by the author(s) under the terms of the Creative Commons Attribution-NonCommercial-NoDerivatives 4.0 International License (CC BY-NC-ND 4.0).

PoS(DISCRETE2020-2021)048

1. Introduction

Measurements of multi-boson productions are essential to establish the existence of gauge self-interaction, including triple gauge coupling and quartic gauge couplings, and deepen our knowledge of the $SU(2)_{\mathrm{L}} \times U(1)_{\mathrm{Y}}$ properties of the electroweak theory. Vector boson scattering (VBS) processes directly probe the gauge unitarity of the Brout-Englert-Higgs mechanism (BEH mechanism) [1, 2]. On the other hand, the multi-boson process opens a promising window for new physics beyond the Standard Model (BSM), such as anomalous triple gauge couplings (aTGC) vertices. In this proceeding, recent ATLAS results on multi-boson productions are presented, including measurements of electroweak production of $Z\gamma$ in association with 2jets, observation of the W pair production in photon-induced collisions as well as the first observation of three W bosons production. Figure 1 shows the representative leading order Feynman digrams contributing to the processed above. Besides, differential measurement of four-lepton cross-sections and combined EFT fit on several differential measurements at ATLAS are also introduced. All the work is based on the collision data collected by the ATLAS detector [3] during Run2 of LHC (2015-2018) with a corresponding integrated luminosity of 139 fb^{-1}.

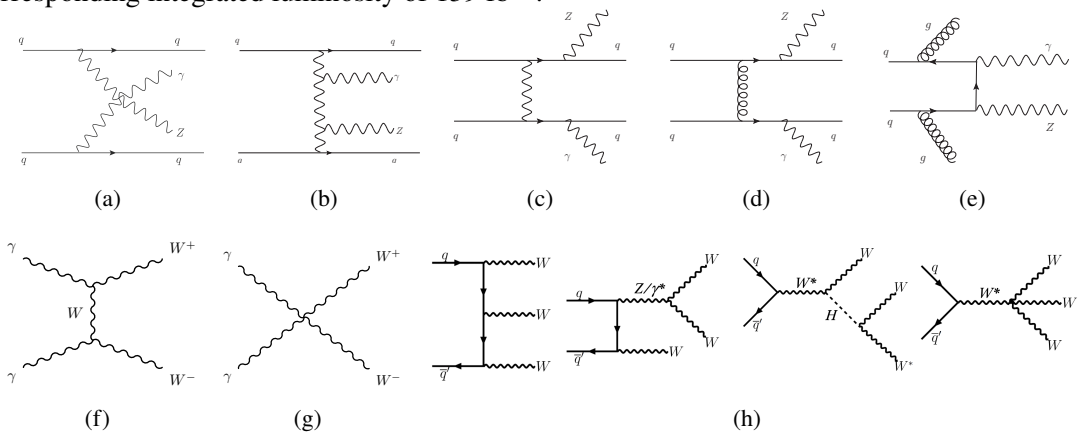

Figure 1: (a) $Z\gamma jj$ quartic gauge coupling; (b) $Z\gamma jj$ triple gauge coupling; (c) $Z\gamma jj$ electroweak non-VBS process; (d) $Z\gamma jj$ gluon exchange; (e) $Z\gamma jj$ gluon radiation; (f) $\gamma\gamma WW$ triple gauge coupling; (g) $\gamma\gamma WW$ quartic gauge coupling; (h) WWW production processes.

2. Observation of the electroweak production of $Z\gamma jj$

This work reports the observation of electroweak production of $Z\gamma$ + 2jets process, which probes the $Z\gamma$ version of VBS. Two decay channels of $Z \to \ell\ell$ and $Z \to \nu\nu$ are studied separately [4, 5]. The final state of $Z\gamma jj$ has contributions from electroweak-induced processes (Process (a), (b) and (c) in Figure 1) as well as QCD-induced processes (Process (d) and (e) in Figure 1). The latter ones are the most dominant background. Topology study has revealed that electroweak processes are associated with more central boson pair and two forward hadronic jets in the opposite hemisphere. A discriminant, centrality, is designed accordingly to enhance the electroweak processes. In charged leptonic Z decay channel, the centrality is defined as in equation 1.

$$\zeta(\ell\ell\gamma) = \left|\frac{y_{\ell\ell\gamma} - (y_{j_1} + y_{j_2})/2}{y_{j_1} - y_{j_2}}\right| \tag{1}$$

in which $y_{\ell\ell\gamma}$ is the rapidity of $Z\gamma$ system, y_j represents the rapidity of jet. Signal region is defined with $\zeta(\ell\ell\gamma) < 0.4$ while in control region $\zeta(\ell\ell\gamma) > 0.4$. Other event selections are detailed in [4].

PoS(DISCRETE2020-2021)048

The post-fit plots of m_{jj} distribution are (a) and (b) in Figure 2 for signal region and control region. Electroweak production is observed with a significance of 10σ (exp. 11σ). The fiducial production cross-section is measured to be 4.49 ± 0.58 fb. For $Z \to \nu\nu$ channel, a similar centrality is defined to condense the electroweak events [5] and the post-fit plot of m_{jj} is (c) in Figure 2. The reported observation significance of electroweak production is 5.2σ (exp. 5.1σ) and the measured fiducial cross-section is 1.31 ± 0.29 fb. Both of them are found to be consistent with SM predictions of 4.73 ± 0.27 fb for $\ell\ell$ channel and 1.27 ± 0.17 fb for $\nu\nu$ channel.

3. Observation of $\gamma\gamma \to WW$ production

In the SM, the $\gamma\gamma \to WW$ process proceeds via triple and quartic gauge-boson interactions (shown in (f) and (g) of Figure 1). This process is special as it involves exclusively the diagrams with self-couplings of electroweak gauge bosons at leading order. The W pairs are selected to decay into opposite-charge $e\mu\nu_e\nu_\mu$. The process is purely electroweak, and the initial protons either stay intact or fragment but with very forward direction. These properties mean the charged particle activity around the vertex is largely suppressed. Hence the strategy to distinguish the signal from background consisting of non-photon collisions is set to select isolated di-lepton vertex with no additional tracks. A large number of data-driven methods are in use for track multiplicity correction as it's badly modelled. The density of pile-up vertices is corrected by a reweighting procedure based on number of tracks sampling from different longitudinal impact parameter z_0. The background prediction distorted by underlying events is corrected with Drell-Yan process measurement. And additional rescattering after initial $\gamma\gamma \to WW$ and dissociative components are corrected by $\gamma\gamma \to \ell\ell$ data [6]. The signal region is defined with $n_{\text{trk}} = 0$ and $p_{\text{T}}^{e\mu} > 30$ GeV, and the rest of $n_{\text{trk}} \otimes p_{\text{T}}$ phase space are treated as control regions as shown in Figure 3. The Background only hypothesis is rejected with significance of 8.4σ (exp. 6.7σ) by simultaneously fit in signal region and control regions. A cross-section of 3.13 ± 0.42 fb is measured in the fiducial volume, while the SM prediction is 2.34 ± 0.27 fb. The difference might be caused by the imprecise data-driven scale factor to correct the additional rescattering mentioned above. More data is needed to pin the effect down. [6].

4. Observation of WWW production

The production channels of WWW are shown in (h) of Figure 1. This work presents the observation of this process at ATLAS [7]. The measurement is done in two channels: 2ℓ channel with two same-sign leptons ($e^\pm e^\pm$, $e^\pm\mu^\pm$, $\mu^\pm\mu^\pm$) as well as at least two jets; 3ℓ channel in which all W bosons decay leptonically with no same-flavor opposite-sign leptons. The background is mainly from WZ process, γ conversion, charge-flip and non-prompt leptons. To classify signal and background, a multivariate technique, Boosted Decision Tree (BDT), is used in 2ℓ and 3ℓ channels respectively. The typcial BDT input variables used are p_T of leptons and jets as well as missing E_T significance etc [7]. A Data-driven approach is applied to scale WZ background (with leptonic W/Z decays) according to jet multiplicity. Figure 4 shows the BDT output distributions in different channels. The signal significance from the fit on BDT output distributions in the signal region and $m_{\ell\ell\ell}$ distributions in WZ control regions finally yields 8.2σ (exp. 5.4σ), indicating the observation of WWW production. The inclusive cross-section is measured to be 820 ± 128 fb, approximately 2.6 standard deviations from the predicted cross section of 511 ± 18 fb. The discrepancy will be further studied with large data sets of ATLAS in future Run3 of LHC. [7]

PoS(DISCRETE2020-2021)048

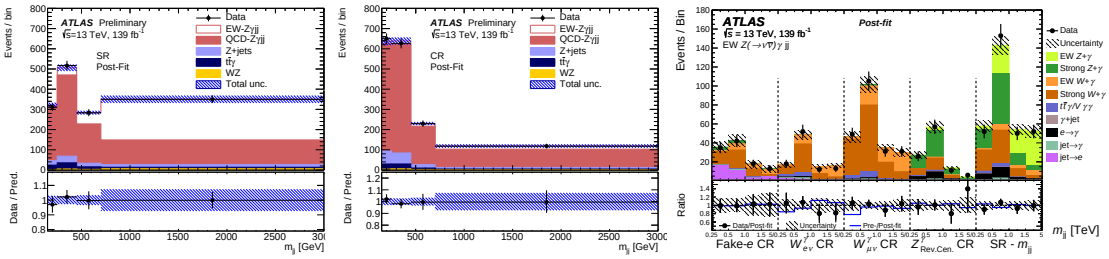

(a) (b) (c)

Figure 2: Post-fit m_{jj} distribution in signal region ($\zeta(\ell\ell\gamma) < 0.4$) (a) and control region ($\zeta(\ell\ell\gamma) > 0.4$) (b) [4]. (c) Post-fit m_{jj} distribution in signal region and control regions for $Z \to \nu\nu$ decay channel [5].

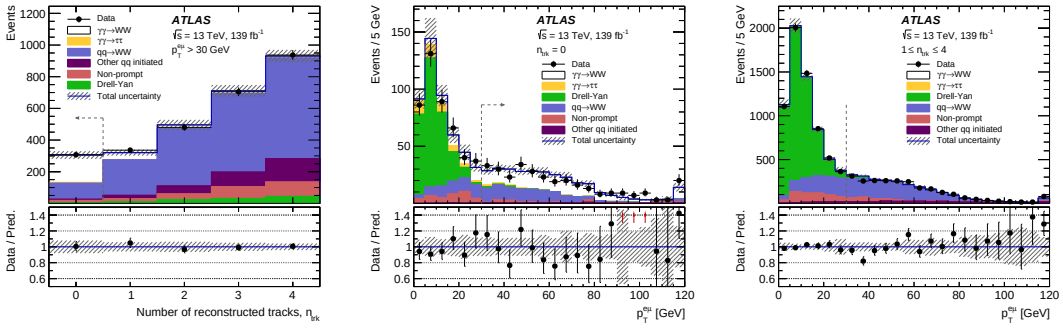

(a) (b) (c)

Figure 3: (a) Distribution of number of tracks n_{trk} associated with the interaction vertex. (b) Distribution of $p_{\text{T}}^{e\mu}$ for $n_{\text{trk}} = 0$. (c) Distribution of $p_{\text{T}}^{e\mu}$ for $1 < n_{\text{trk}} < 4$. [6]

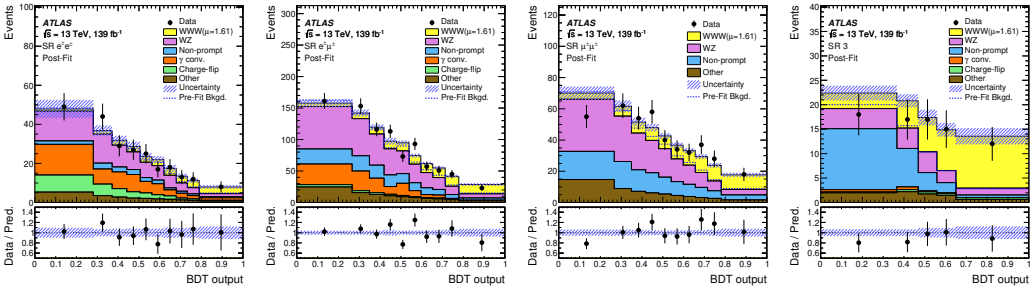

(a) (b) (c) (d)

Figure 4: (a) BDT output in $e^{\pm}e^{\pm}$ channel. (b) BDT output in $e^{\pm}\mu^{\pm}$ channel. (c) BDT output in $\mu^{\pm}\mu^{\pm}$ channel. (d) BDT output in 3ℓ channel. [7]

5. Measurement of four-lepton differential cross-sections and BSM interpretations

This work performs the differential cross-section measurement on inclusive four-lepton events as a function of various observables [8]. The aim is to get precise and inclusive measurement results so as to provide rich material for SM testing and BSM interpretation. Figure 5(b) shows the measured differential cross-section of $m_{4\ell}$. Two examples of BSM models are interpreted in this work. Firstly 22 Wilson coefficients of SMEFT dim-6 operators are constrained, covering

PoS(DISCRETE2020-2021)048

effects on Higgs coupling, gauge boson couplings, 4-fermion interactions etc. The observables are scanned respectively to match the most sensitive operators, on which the limit is set. Figure 5(a) summarizes the limit of each individual operator. Another interpretation is applied on B-L model, which introduces a local $U(1)_{\text{B-L}}$ gauge symmetry with coupling constant g'. The model predicts a Z' and an exotic Higgs boson h_2, from the spontaneously symmetry breaking, that mixes with the SM Higgs, with a mixing angle α [8]. Differential cross-sections provide 2D parameter limits of the model, shown in Figure 5(c).

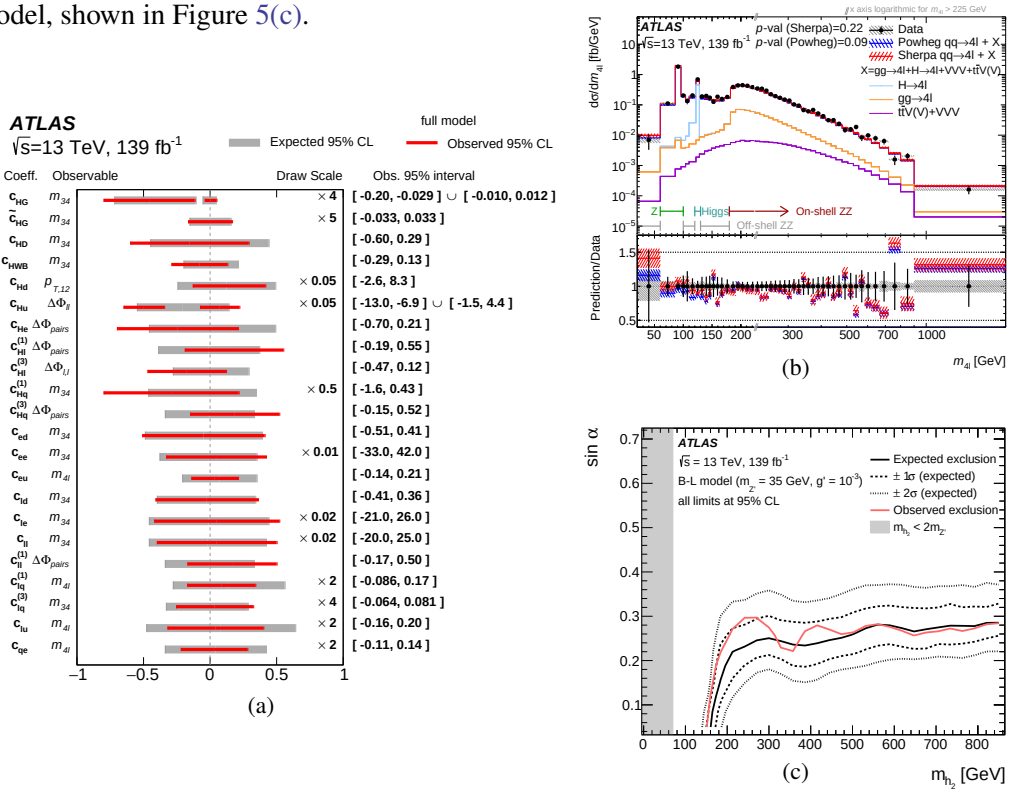

Figure 5: (a) Confidence intervals at 95% CL for SMEFT Wilson coefficients. (b) Differential cross-sections as a function of $m_{4\ell}$. (c) Exclusion contour at 95% CL for B-L model in the plane of sinα versus m_{h_2} for $m_{Z'} = 35$ GeV and $g' = 10^{-3}$. [8]

6. Combined EFT fit with ATLAS boson differential measurements

In the field of EFT interpretation, a global fit that combines different analysis results is one of the most important way to improve the constraint power to EFT operators. This work shows an example of performing a global fit with 4 differential measurements at ATLAS [9]. The measurements include differential cross-section of WW, WZ and VBF Z + 2jets production with leptonic decay as well as inclusive four-lepton final states as introduced in Section 5. SMEFT dim-6 operators are considered and 33 Warsaw basis coefficients are tested. To combine different results, experimental uncertainties and their correlation are studied in detail when constructing the likelihood fitting function [9]. The EFT limit setting is done simultaneously on all selected EFT operators, which is achieved with Principal Component Analysis (PCA). The linear combinations of Warsaw basis operators with the most significant sensitivity to the measurements are selected. Finally 15 sensitive directions in parameter space are constrained. Both linear model (only the contributions from the interference of SM and EFT included) and full model (all contributions from EFT included) are

PoS(DISCRETE2020-2021)048

considered to estimate uncertainties due to the truncation of the EFT expansion. The confidence intervals for EFT parameters are listed in Figure 6.

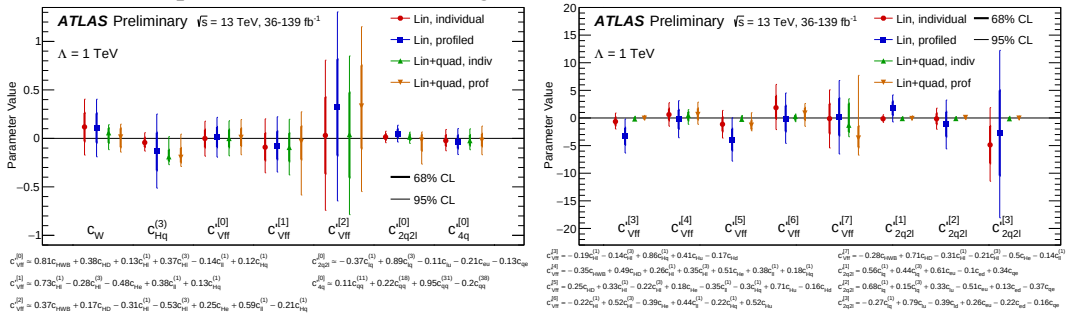

Figure 6: Confidence intervals for the 15 parameters included in the combined fit [9]

7. Summary

This proceeding summarizes recent ATLAS multi-boson analyses, in which the observation of VBS $Z\gamma$ production, WWW process, as well as $\gamma\gamma \to WW$ scattering are presented. Also differential measurement of inclusive 4ℓ production and limit setting on Wilson coefficients of SMEFT by a combined fit to several multi-boson cross-section measurements are included.

References

[1] F. Englert and R. Brout, *Broken Symmetry and the Mass of Gauge Vector Mesons*, *Phys. Rev. Lett.* **13** 321.

[2] Peter Higgs, *Broken Symmetries and the Masses of Gauge Bosons*, *Phys. Rev. Lett.* **13** 508.

[3] ATLAS Collaboration, *The ATLAS Experiment at the CERN Large Hadron Collider*, *JINST* **3** (2008) S08003.

[4] ATLAS Collaboration, *Measurement of the cross-section of the electroweak production of a $Z\gamma$ pair in association with two jets in pp collisions at $\sqrt{s} = 13$ TeV with the ATLAS detector*, *ATLAS-CONF-2021-038*, URL: http://cdsweb.cern.ch/record/2779171.

[5] ATLAS Collaboration, *Observation of electroweak production of two jets in association with an isolated photon and missing transverse momentum, and search for a Higgs boson decaying into invisible particles at 13 TeV with the ATLAS detector*, *Eur. Phys. J. C* **82** 2 (2022) 105.

[6] ATLAS Collaboration, *Observation of photon-induced W^+W^- production in pp collisions at $\sqrt{s} = 13$ TeV using the ATLAS detector*, *Phys. Lett. B* **816** (2021) 136190.

[7] ATLAS Collaboration, *Observation of WWW production in pp collisions at $\sqrt{s} = 13$ TeV with the ATLAS detector*, *arXiv:2201.13045*, URL: https://arxiv.org/abs/2201.13045.

[8] ATLAS Collaboration, *Measurements of differential cross-sections in four-lepton events in 13 TeV proton-proton collisions with the ATLAS detector*, *JHEP* **5** (2021).

[9] ATLAS Collaboration, *Combined effective field theory interpretation of differential cross-sections measurements of WW, WZ, 4ℓ, and Z-plus-two-jets production using ATLAS data*, *ATL-PHYS-PUB-2021-022*, URL: http://cdsweb.cern.ch/record/2776648.

PoS(DISCRETE2020-2021)048